

TRANSPORTATION POOLED FUND PROGRAM QUARTERLY PROGRESS REPORT

Lead Agency (FHWA or State DOT): Kansas DOT

INSTRUCTIONS:

Project Managers and/or research project investigators should complete a quarterly progress report for each calendar quarter during which the projects are active. Please provide a project schedule status of the research activities tied to each task that is defined in the proposal; a percentage completion of each task; a concise discussion (2 or 3 sentences) of the current status, including accomplishments and problems encountered, if any. List all tasks, even if no work was done during this period.

Transportation Pooled Fund Program Project # TPF-5(328)	Transportation Pooled Fund Program - Report Period: <input type="checkbox"/> Quarter 1 (January 1 – March 31) <input type="checkbox"/> Quarter 2 (April 1 – June 30) <input type="checkbox"/> Quarter 3 (July 1 – September 30) <input checked="" type="checkbox"/> Quarter 4 (October 1 – December 31)	
Project Title: Strain-based Fatigue Crack Monitoring of Steel Bridges using Wireless Elastomeric Skin Sensors		
Project Manager: Susan Barker, P.E. Phone: (785) 291-3847 E-mail: SusanB@ksdot.org		
Project Investigator: Li Jian Phone: 785-864-6850 E-mail: jianli@ku.edu		
Lead Agency Project ID: RE-0699-01	Other Project ID (i.e., contract #): _____	Project Start Date: 9/2015
Original Project End Date: Multi-year project	Current Project End Date: 8/31/2018	Number of Extensions: N.A.

Project schedule status:

- On schedule
 On revised schedule
 Ahead of schedule
 Behind schedule

Overall Project Statistics:

Total Project Budget	Total Cost to Date for Project	Total Percentage of Work Completed
\$405,000	\$ 122,585.79	40%

Quarterly Project Statistics:

Total Project Expenses This Quarter	Total Amount of Funds Expended This Quarter	Percentage of Work Completed This Quarter
\$ 23,695.70	\$ 23,695.70	7%

Project Description:

The main objective of this proposed research is to *provide state DOTs a practical and cost-effective long-term fatigue crack monitoring methodology using a **wireless elastomeric skin sensor network***. This research is intended to demonstrate the value-added of fatigue crack monitoring of steel bridges using wireless skin sensors over the traditional bridge inspection.

Progress this Quarter (includes meetings, work plan status, contract status, significant progress, etc.):*ISU Progress:*

Under this task, fatigue crack sensors are to be produced with an approximate thickness of 100-200 μm to enhance the mechanical robustness under harsh environment. Acceptable range of capacitance is 800-1000 pF. The anticipated number of sensors is 150 to 200 for the duration of the project.

A meeting occurred on October 7th during which it was agreed to start fabricating a different geometry (1" x 1"). The production has started in October, and 45 sensors have been delivered in December. Technical support (Task 3) is being provided to KU on a continuous basis, as well as discussion and feedback (Task 4).

KU Progress:

KU team carried out two tasks in this quarter: testing the sensors performance under threshold stress intensity for fatigue crack growth and further investigation under a more realistic traffic loading.

UA Progress:

Arizona team has been focused on improving the performance of the capacitive strain sensor board particularly when used with large-size (e.g. 2 in x 2 in) SEC sensors. Associated challenge is due to its high-value nominal capacitance and low sensitivity that require high gain (signal amplification) for the signal from SEC sensor. Higher gain may cause higher noise and signal clip (saturation). Particularly, unexpected signal clip happened in the first stage signal amplification. The reason for the signal clip has been identified. The input signal to the amplifier should be limited within the range of 1 ~ 3V, particularly when AC input (instead of DC) is fed, even though 5V power supply is used for the amplifier. To resolve this issue, a common-mode DC voltage has been provided for both positive & negative inputs such that the amplifier does not exceed the range limit. The sensor board has been modified accordingly.

Anticipated work next quarter:

ISU: Production of sensors will continue in the next quarter. Technical support (Task 3) is being provided to KU on a continuous basis, as well as discussion and feedback (Task 4).

KU: KU will continue to run the threshold test by increasing the loading to further grow the crack until the specimen reaches complete failure. The sensor will be tested with large-scale bridge specimens in the structures laboratory. Programing of the Xnodes to enable autonomous monitoring will begin in this quarter.

UA: In the next quarter, Arizona team will continue to improve the performance of the sensor board particularly with large SEC sensor, and will start to design interface board for the sensor board to be used with Xnode.

Significant Results:

Part 1: Crack detection using SEC sensor

KU team performed two tasks in this quarter: the threshold test and further investigation under more realistic traffic loading.

1. Threshold test

The purpose of the threshold test is to evaluate the SEC sensor's performance when the stress intensity for fatigue crack growth is approaching its threshold. Same test setup is adopted as previous tests, as shown in Fig. 1. The SEC sensor is attached to the surface of a small-scale compact specimen and the fatigue load is applied through the Instron uniaxial loading frame. To ensure that the fatigue crack growth can reach its threshold in the test, we designed a new loading protocol shown in Fig. 2. The design principle is to continuously decrease the range of stress intensity factor (ΔK), allowing ΔK to approach the threshold, such that the performance of the SEC sensor under such a particular loading can be evaluated. In particular, we assign the initial ΔK as $20 \text{ ksi in}^{1/2}$, which decreases by $2 \text{ ksi in}^{1/2}$ for every $3/16 \text{ in.}$ of crack growth. For instance, ΔK starts at $20 \text{ ksi in}^{1/2}$ and decreases to $18 \text{ ksi in}^{1/2}$ when the crack reaches $3/16 \text{ in.}$

At the time of writing this report, the test has been running for two months. The latest update about the test is that the crack stopped growing at $24/16 \text{ in.}$ (1.5 in.) after the ΔK was dropped to $4 \text{ ksi in}^{1/2}$. Then, we applied about 3 million cycles and took a number of measurements (results will be shown in later section of this report). Our next testing plan is to resume the crack growth by increasing the ΔK , as shown in the last stage of Fig. 2.

To verify the crack monitoring ability of the SEC sensor, we adopt the same data processing technique as previous tests. Fig. 3 shows a flow chart of the data processing method. Briefly, a series of short period of measurements of the SEC sensor C_i and load F_i are taken during the fatigue testing when the crack reaches different lengths. Frequency analyses are performed by to compute the power spectral densities (PSDs) of these measurements. The ratio between the PSD peaks of the sensor and the load is calculated as the crack growth indicator (CGI). The fatigue crack growth can be successfully identified by increased CGIs.

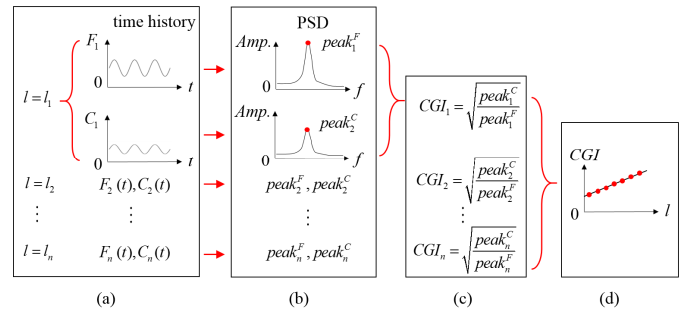
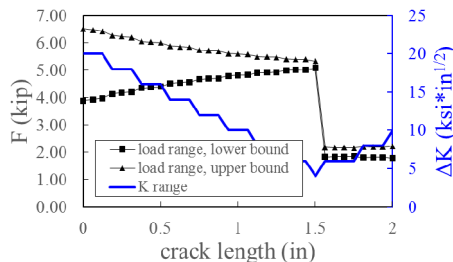


Fig. 1 Test setup

Fig. 2 Loading protocol of the threshold test

Fig. 3 Proposed data processing method

The threshold testing results are shown in two parts. We first illustrate the testing results prior to the crack stop, showing the ability of the SEC sensor for crack growth monitoring. In the second part, we use the data points taken when the crack is under the threshold stress intensity.

Fig. 4 shows the CGIs vs. crack length prior to the crack stop. Each data point on the plot corresponds to a measurement when the crack reaches each additional $1/16 \text{ in.}$ Fig. 5 shows the same CGIs vs. number of loading cycles. The vertical axes of both figures are in log scale. The result clearly indicates that CGI increases when the crack grows further. The crack length in Fig. 4 is the physical crack length in the specimen measured from the notch to the crack tip; however, the effective sensing area is $5/16 \text{ in.}$ away from the notch, as shown in Fig. 6. The red dash lines in Fig. 4 and Fig. 5 indicate the moment when the crack reaches the edge of the sensing area.

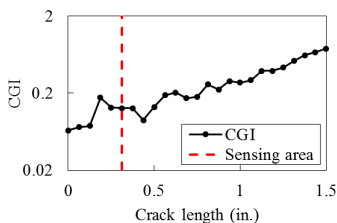


Fig. 4 Crack growth indicator (CGI) vs. crack length

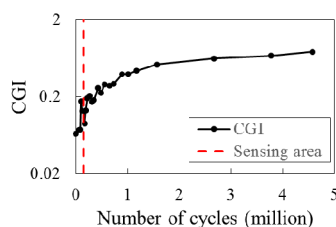


Fig. 5 Crack growth indicator (CGI) vs. number of cycles

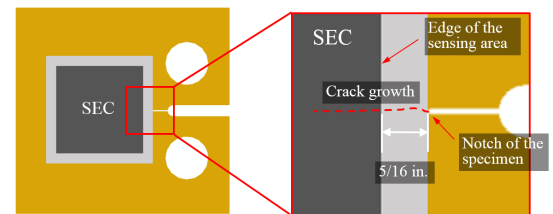


Fig. 6 Demonstration of the boundary of the sensing area

Fig. 7 shows all CGI data points including the ones taken during the period when the crack stopped growing (last 10 data points shown in Fig. 7). The history of ΔK is also shown in the same figure (blue line). During the testing, crack growth rate became very slow under $\Delta K = 6 \text{ ksi in}^{1/2}$. The crack took about 0.8 to 1.1 million cycles to grow additional 1/16 in. Then we dropped ΔK to $4 \text{ ksi in}^{1/2}$ and found that the crack nearly stopped growing at 24/16 in., although later we found the crack grew to 25/16 in. after about 2.5 million cycles. Under $\Delta K = 4 \text{ ksi in}^{1/2}$, we took 5 measurements with an increment of 0.2 million cycles. Next, we further dropped ΔK to $2 \text{ ksi in}^{1/2}$ and took 5 additional measurements with same increment. Results in Fig. 7 indicate the CGIs stay relatively constant within a limited range when the crack stopped growing.

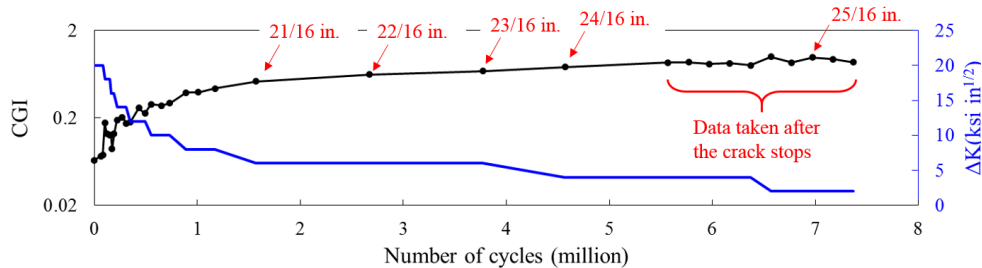


Fig. 7 CGI before and after the crack growth stops

2. Further investigation of traffic load

In the last quarterly report, we showed preliminary work for investigation of realistic traffic load. In this quarter, we modified the traffic loading and verified the sensor's performance using the threshold test.

Fig. 8 shows the modified traffic loading. It contains 20 cycles of sinusoid, but each cycle of sinusoid has different statistic features in terms of peak-to-peak amplitude and frequency. The design principle is to vary these two important features for each load cycle to reflect more realistic statistic features of traffic loads of steel bridges.

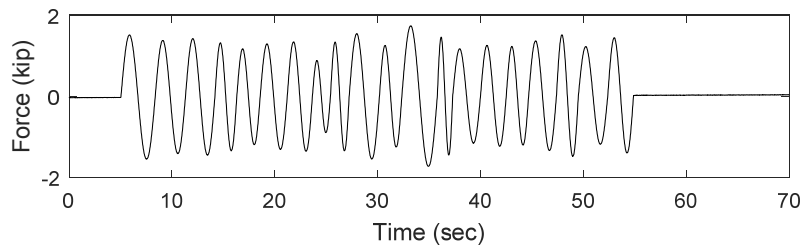


Fig. 8 Modified traffic load

For one particular load cycle in steel bridges, the peak-to-peak amplitude is governed by the weight of the vehicle. Based on references in the literature, we found among all types of vehicles, full-loaded heavy trucks are the main sources that would induce the fatigue crack growth. The probability distribution of such groups of heavy trucks can be simplified as a normal distribution with a coefficient of variation (COV) of 0.22. However, for the purpose of laboratory test, a lower COV of 0.11 is applied for the loading design for the safety concern of the specimen. Meanwhile, the frequency of the load cycle is governed by multiple factors including vehicle speed and bridge span lengths. Among of these two factors, we decided to focus on vehicle speed by introducing a COV of 0.18 based on literature.

As a results, we designed the traffic load with 20 cycles, shown in Fig. 8. The frequencies of all load cycles are subject to a normal distribution with a mean of 0.42 Hz and a COV of 0.18. For the peak-to-peak amplitudes, a lower COV of 0.11 is assigned for the safety concern of the test as mentioned previously. The mean peak-to-peak amplitude is determined by the ΔK , as shown in Fig. 2.

We utilized the threshold test to verify the sensor's performance under the modified traffic load. When the crack grows additional 1/16 in., we apply the traffic load (Fig. 8) to the specimen and take the measurement of the sensor and the load. Then, the data processing strategy shown in Fig. 3 is applied to compute the CGIs. Finally, the results of CGIs vs. crack length under the modified traffic load is shown in Fig. 9.

Fig. 9 demonstrates that the sensor is able to monitor the crack growth by producing an increasing CGI. This is consistent with our preliminary investigation and indicates that the proposed data processing method works when the specimen is subjected to a more realistic traffic load.

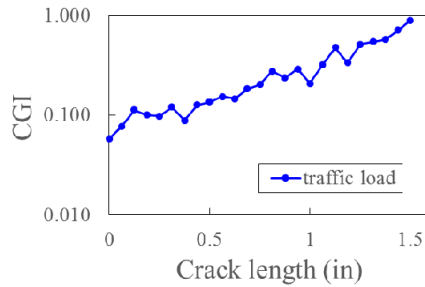
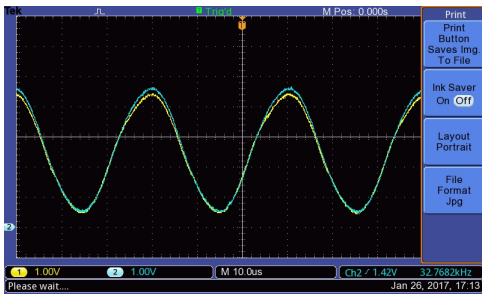


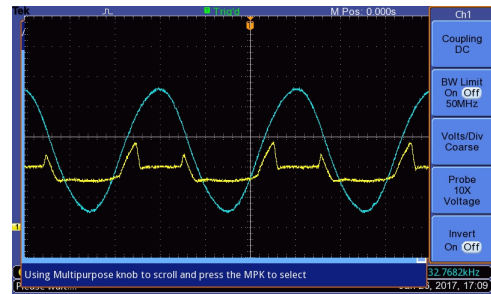
Fig. 9 CGI vs. crack length under the modified traffic loading

Part 2: Wireless data acquisition

Signal clip (saturation) happened at the amplifier under high input level. Fig. 1(a) shows two signals from both sides of the Wheatstone bridge arms and Fig. 1(b) shows a signal from one side of Wheatstone bridge arm (blue line) and the amplified signal from the other side of the bridge arm (yellow line). The amplified signal in Fig. 1(b) shows clipped shape which is due to signal exceeding 3V limit. Fig. 2 shows the input common-mode voltage range for the amplifier with +5V power supply, which should be -1V ~ 3V to have amplified output between 0 and 5V (from Datasheet of the AD8220 amplifier).



(a) Blue : Reference side, Yellow : Sensor side



(b) Blue : reference side Yellow : Amplified signal

Fig. 1. Wheatstone bridge output signal

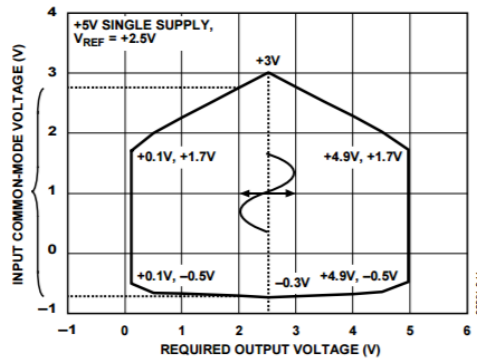


Fig. 2. AD8220 Required Output Voltage vs. Common-Mode Input Voltage

To resolve this issue, the amplifier input is modified by applying a DC common-mode voltage, V_{cm} . Fig. 3 shows the modified circuit diagram, with the DC common-mode voltage supply shown in the blue box. V_{cm} directly acts as average voltage of signals. The values of resistors and capacitors are selected accordingly to ensure the signals fit the range shown in Fig. 2.

Fig. 4. Shows signals from the modified sensor board. Input voltage range has been adjusted by providing 1V as V_{cm} that makes the range between 0V and 2V, as shown in Fig. 4(a). Fig. 4(b) shows the amplified signal without clip. Effort is being made to achieve larger gain and better balance with the modified sensor board.

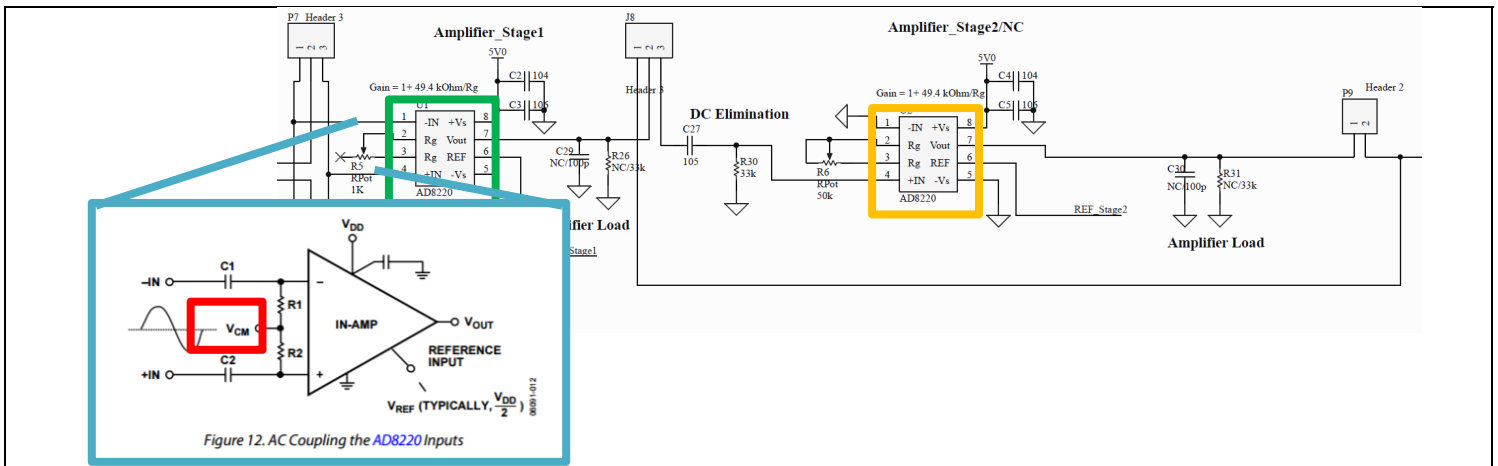
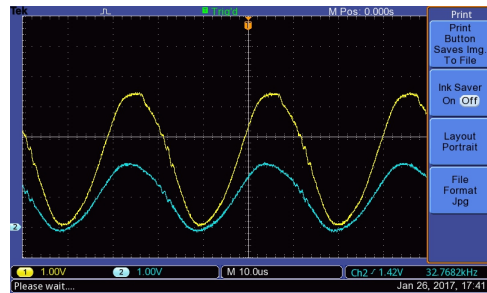
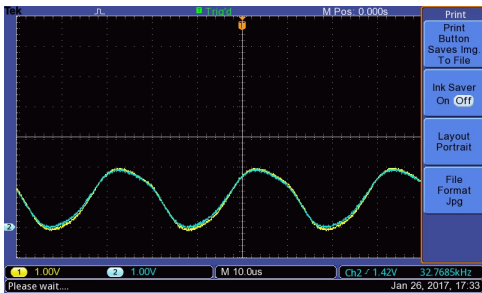


Fig. 3 Modified input section



(a) Blue : Reference side, Yellow : Sensor side (b) Blue : Reference side Yellow : Amplified signal
Fig. 4. Modified Wheatstone bridge output signal

Circumstance affecting project or budget. (Please describe any challenges encountered or anticipated that might affect the completion of the project within the time, scope and fiscal constraints set forth in the agreement, along with recommended solutions to those problems).

None.